TOPOLOGY PROCEEDINGS
Volume 40, 2012
Pages 73–81
http://topology.auburn.edu/tp/

An Upper Semi-Continuous Model for the Lorenz Attractor

by

Benjamin Marlin

Electronically published on May 18, 2011

Topology Proceedings

Web: http://topology.auburn.edu/tp/
Mail: Topology Proceedings
Department of Mathematics & Statistics
Auburn University, Alabama 36849, USA
E-mail: topolog@auburn.edu
ISSN: 0146-4124

http://topology.auburn.edu/tp/

TOPOLOGY PROCEEDINGS
Volume 40 (2012)
Pages 73-81

E-Published on May 18, 2011

AN UPPER SEMI-CONTINUOUS MODEL FOR THE LORENZ ATTRACTOR

BENJAMIN MARLIN

Abstract. In examining the Poincaré map of the Lorenz system, a multi-valued map is suggested by numerical work. We examine the inverse limit of this and related maps in trying to understand the structure of the attractor.

1. Introduction

In considering the Poincaré map of the Lorenz system

$$\frac{dx}{dt} = \sigma(y - x)$$
$$\frac{dy}{dt} = x(\rho - z) - y$$
$$\frac{dz}{dt} = xy - \beta z$$

an interesting Ruelle plot is encountered in the vicinity of the non-zero critical points, as shown in Figure 1. In [8], the values of $\sigma = 10$, $\beta = \frac{8}{3}$, and $\rho = 28$ were used, and many investigators use these values of σ and β while varying ρ. In [3], the form of a first return map on the interval is derived from considerations of the branched manifold. Numerical experimentation suggested a clear set of curves in the Ruelle plot with $\rho = 30$, which is the value we have used.

The restriction of r^2 to $[-p, p]$, where $p \approx 8.79$, suggests a graph which is set-valued, and all the image sets appear to be finite. If we assume that this numerical result approximates a union of arcs, we may analyze the inverse limit of r^2 in the interval, and this will give us an approximation of

2010 *Mathematics Subject Classification.* Primary 54C60; Secondary 37B45.
Key words and phrases. inverse system, Poincaré map, set-valued map.

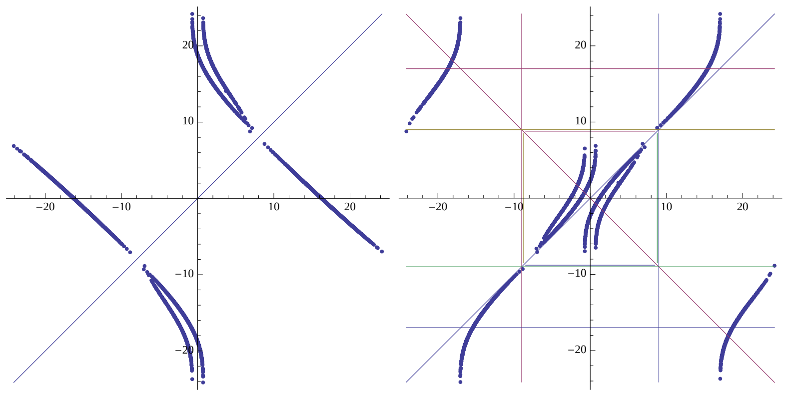

FIGURE 1. The Ruelle plot r on the left. As the Poincaré map is not a self-map, we examine r^2 on the right as well. Note the inner partition of $[-p, p]$.

the attractor. In [7], such an analysis was carried out with a continuous, single-valued map. This approach was suggested by a comment in [2] that the unstable manifold theorem gives a map from the stable manifold of a fixed point back to itself and that the unstable manifold does the same for the inverse. In this case, the function in question is the Poincaré map for the flow of the Lorenz system. In this paper, we examine the inverse system given by analyzing a set-valued function. In using a set-valued function, we are attempting to examine the map from both manifolds to themselves through the projection onto one axis. Our tool allows the maps to be interchanged, however, yielding an interesting inverse limit.

2. Definitions

By a *flow* on an $\mathbb{R}^n$ associated with a system of differential equations, we mean a function $\varphi : \mathbb{R}^n \times \mathbb{R} \to \mathbb{R}^n$ so that $\varphi_t(x) = \phi(t)$ is the unique solution of the system so that $\phi(0) = x$. Under certain conditions, we may choose $S \subset \mathbb{R}^n$ so that for each $s \in S$ there exists $\tau(x) > 0$ so that $\varphi_{\tau(x)}(s) \in S$. In this case, we call S the *Poincaré section* for the flow and define the *Poincaré map* $P : S \to S$ by $P(s) = \varphi_{\tau(x)}(s)$.

For a flow with a Poincaré map $P : S \to S$, we may define a *Ruelle plot* as follows. Let $s \in S$ and $x_k \in \mathbb{R}^n$ be given by $x_k = P^k(s)$ for each $k \in N \subset \mathbb{N}$. We pick one coordinate $j \in \{1, ..., n\}$ and define a collection $\hat{r} = \{(\pi_j(x_k), \pi_j(x_{k+1}) | k \in N\}$. If N is a relatively large set (and especially if x_0 is chosen near an attractor), the image traced out by $\hat{r}$ may suggest a function $\check{r} : \mathbb{R} \to \mathbb{R}$, having the semi-conjugacy $\pi_j \circ P|_S = \check{r} \circ \pi_j$.

A *set-valued function* on X is a function $f : X \to 2^X$. We will work with such set-valued functions which are *upper semi-continuous* (*u.s.c.*) *maps*. While a more technical definition is available, we will use the equivalency, shown in [6], which is to say: A set-valued function f on X such that $f^{-1}(x)$ has finitely many components for each $x \in X$ and $\{(x, y)|x \in X, y \in f(x)\} \subset X \times X$ is closed.

For a function $f : X \to X$, the *inverse limit*, $\varprojlim\{X, f\}$ is a set $M \subset \prod_{n\in\mathbb{N}} X$ so that $x \in M$ provided that $\pi_n(x) = f \circ \pi_{n+1}(x)$ for all $n \in \mathbb{N}$. A subject of recent interest has been to replace the function with a u.s.c. map. Where the distinction is important, we will refer to a *u.s.c. inverse limit* with a u.s.c. map $f : X \to 2^X$ as the set $M \subset \prod_{n\in\mathbb{N}} X$ so that $x \in M$ provided that $\pi_n(x) \in f \circ \pi_{n+1}(x)$.

Frequently, we refer to a Cantor set, using the standard definition. Since we are here considering the canonical "middle-thirds" Cantor set, we have chosen to represent this as $\mathcal{C}$ throughout.

3. Inverse Limit Results for the Simplest Model

An initial attempt at a model for this system might follow the technique of [7] in approximating each paired branch of the Ruelle plot with a single curve. For simplicity, we first approach this with piecewise linear maps β_m for $m \geq 0$. Let $I = [0, 1]$ and define $\beta_m : I \to 2^I$ to be the union of the lines with slope m through the points $(0, 0)$ and $(1, 1)$. We may express this algebraically for $1 < m \leq 2$ as

$$\beta_m(x) = \begin{cases} \{mx\} & \text{if } x < 1 - \frac{1}{m} \\ \{mx, mx - m + 1\} & 1 - \frac{1}{m} \leq x \leq \frac{1}{m} \\ \{mx - m + 1\} & x > \frac{1}{m}. \end{cases}$$

Although the Ruelle plot technique suggests a connection for which $m > 1$, we may extend the definition of the family for $0 \leq m < 1$ by $\beta_m(x) = \{mx, mx - m + 1\}$. (See Figure 2.) An immediate observation may be made about the inverse limits of these maps for which $m > 1$.

Lemma 3.1. *Let $m > 1$ and $f : [0, 1] \to [0, 1]$ be a function so that $f(x) = mx$ for $x \leq \frac{1}{m}$. Then $M = \varprojlim\{[0, 1], f\}$ contains an arc.*

Proof. Let $x \in [0, \frac{1}{m}]$. Then $(x, \frac{x}{m}, \frac{x}{m^2}, ...) \in M$ as well. This establishes a continuous image of $[0, \frac{1}{m}]$ in M. □

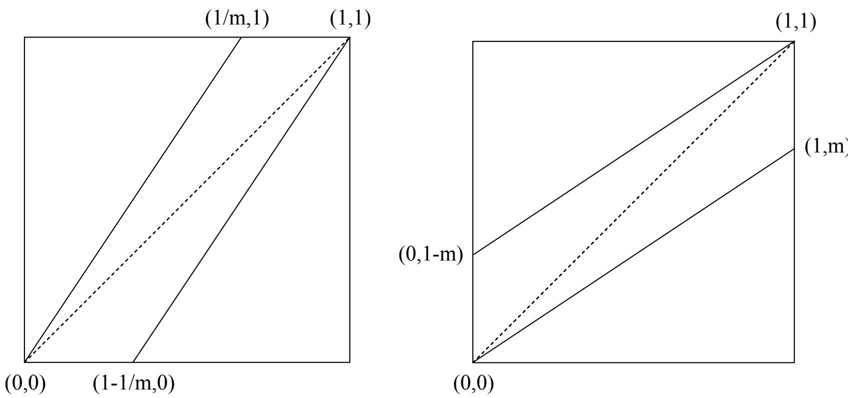

FIGURE 2. Members of the family of u.s.c. maps β_m : $[0,1] \to 2^{[0,1]}$ for $m > 1$ (left) and $m < 1$ (right).

Lemma 3.1 and its proof are a simple observation made in [5], but we have separated them here for reference. The proof, while trivial, suggests a more general statement, as the critical detail is simply that $\dfrac{x}{m^n}$ vanishes as $n \to \infty$.

Lemma 3.2. *Let I be an arc with endpoint a and let J be a subcontinuum of I containing a. Let $f : I \to I$ be a function so that $f|_J$ is a homeomorphism with a being the only fixed point of f in J. If there exists $b \in J$ so that $(f^{-1})^n(b) \to a$ as $n \to \infty$, then $\varprojlim\{I, f\}$ contains an arc.*

Proof. This follows from the proof of Lemma 3.1 by simply replacing $\frac{x}{m^n}$ with $\left(f^{-1}\right)^n(x)$. □

Consequently, we may conclude that $\varprojlim\{I, \beta_m\}$ contains an arc, and an argument from symmetry implies that it contains a pair of symmetric arcs. In a similar vein, we may expect $\lim\{[-p,p], r^2\}$ to contain such a pair of arcs as well. Unfortunately, although more general, this is a relatively uninteresting result. Specificity allows us to say more.

Proposition 3.3. *For $1 < m \leq 2$, $\mathcal{M}_m = \varprojlim\{I, \beta_m\}$ is homeomorphic to the product of an arc and a Cantor set.*

Proof. This proceeds much in the manner of [1] and [4], with the appropriate adjustments for a u.s.c. map. We define a new u.s.c. map $B_m : I \times I \to 2^{I \times I}$ so that $B(x_1, x_2)$ is a two-element set if $1 - \frac{1}{m} \leq x \leq \frac{1}{m}$ and a one-element set otherwise (this should sound familiar). If

$x_2 < 1 - \frac{1}{m}$, let $B_m(x_1, x_2) = \left\{\left(\frac{x}{3}, mx\right)\right\}$. Symmetrically, if $x_2 > \frac{1}{m}$, define $B_m(x_1, x_2) = \left\{\left(\frac{x+1}{3}, mx - m + 1\right)\right\}$. For $1 - \frac{1}{m} \le x \le \frac{1}{m}$, define $B_m(x_1, x_2) = \left\{\left(\frac{x}{3}, mx\right), \left(\frac{x+1}{3}, mx - m + 1\right)\right\}$. For ease of reference, this is represented by Figure 3.

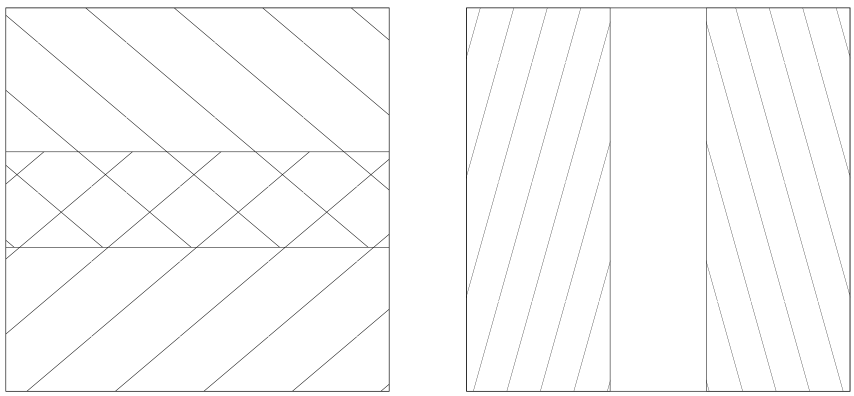

FIGURE 3. On the left, the pre-image $I \times I$, with hashing added to distinguish the regions. On the right, the image under B_m.

We have constructed B_m to be semi-conjugate to β_m using the projection onto the x_2 axis. As $n \to \infty$, the width of individual images of foliations of $I \times I$ goes to zero, so that the semi-conjugacy, acting on the attracting set $\mathcal{B}_m = \cap_{n>0} B_m^n(I \times I)$, becomes a conjugacy. Consequently, the attracting set of $I \times I$ under B_m is homeomorphic to $\mathcal{M}_m$. □

As a differentiable flow is a reversible system, we might also want to examine the inverse limit of $\left(r^2\right)^{-1}$. The map β_m for $m < 1$ is actually easier to work with and the same techniques apply. Due to the symmetry of inverses, we find that $\beta_m^{-1} = \beta_{\frac{1}{m}}$. It is interesting to note that, for $m \ge \frac{1}{2}$, the map is a surjection and we can be assured that the inverse limit exists. A cursory inspection might suggest that, since the situation of Lemma 3.1 is reversed, we could expect only a trivial inverse limit. This is not quite true.

Proposition 3.4. *For $m < \frac{1}{2}$, $\mathcal{M}_m = \varprojlim\{I, \beta_m\}$ is homeomorphic to a Cantor set.*

Proof. Applying the technique of Proposition 3.3, but with $m < 1$, we create two images of $I \times I$: $\left[0, \frac{1}{3}\right] \times [0, m]$ and $\left[\frac{2}{3}, 1\right] \times [1 - m, 1]$. We find that $\pi_2 \circ B_m(I \times I)$ is separated into two intervals, and thus that $\pi_2 \circ \mathcal{B}_m$ will be a Cantor set, just as $\pi_1 \circ \mathcal{B}_m$ is. □

Remark 3.5. For $m > \frac{1}{2}$, $\pi_2(\mathcal{M}_m) = I$ as each image $\pi_2 \circ B_m^n(I \times I) = I$.

Remark 3.6. For $\frac{1}{2} \leq m < 1$, $\mathcal{M}_m$ must not contain any arcs, as $B_m(\mathcal{B}_m)$ contracts vertically. But since $\pi_2 \circ B_m^n(I^2) = I$, $\pi_2(\mathcal{B}_m) = I$, as well.

Remark 3.7. We have neglected the case $m = 1$, as there $\beta_m = id$, meaning the inverse limit is simply an arc.

4. More Complex Models

When we have committed to the use of set-valued maps, such as β_m, it seems a relatively small step to extend this to what may be a more robust model. Let $a \in I$ be chosen so that $a \approx \frac{1}{2}$ (this specification may seem somewhat arbitrary—it is intended to create a model which closely resembles the observed plots). Define $\tilde{\beta}_a : I \to 2^I$ as the union of four line segments: the segment through (0,0) and $(a, 1)$, the segment through (0,0) and $(1-a, 1)$, the segment through (1,1) and $(a, 0)$, and the segment through (1,1) and $(1-a, 0)$. This may be described algebraically as

$$\tilde{\beta}_a(x) = \begin{cases} 0 & \text{if } x = 0 \\ \{\frac{x}{a}, \frac{x}{1-a}\} & \text{if } 0 < x < a \\ \{\frac{x}{1-a}, \frac{x-a}{1-a}\} & \text{if } a \leq x \leq 1-a \\ \{\frac{x-a}{1-a}, \frac{x-(1-a)}{a}\} & \text{if } 1-a < x < 1 \\ 1 & \text{if } x = 1. \end{cases}$$

A further—and much more general—step would be to consider a union of four twice-differentiable curves $\hat{g} = g_1 \cup g_2 \cup g_3 \cup g_4$ on [0,1] with the same endpoints so that $g_1(0) = g_2(0) = 0$, $g_1'(0) > g_2'(0) > 1$, $g_1''(x), g_2''(x) > 0$, $g_3(x) = g_1(1-x)$, and $g_4(x) = g_2(1-x)$. (See Figure 4.) These are designed to mimic the symmetry of r^2 and to satisfy the conditions of the following.

Theorem 4.1. *Let I be an arc with an endpoint a and let J be a subcontinuum of I containing a. Let $f : I \to 2^I$ be a semicontinuous function such that $f|_J$ consists of the union of two homeomorphisms f_0 and f_1 so that each of $\varprojlim\{I, f_k\}$ contains an arc. Then $M = \varprojlim\{I, f\}$ contains a cone over a Cantor set.*

Proof. Let c be the binary representation of a point of the canonical middle-thirds Cantor set, $\mathcal{C}$, and let $x \in J$. Construct $m(x, c) \in M$ by taking $m_0 = x$ and $m_n = f_{c_n}^{-1}(m_{n-1})$. As each f_k is a surjective

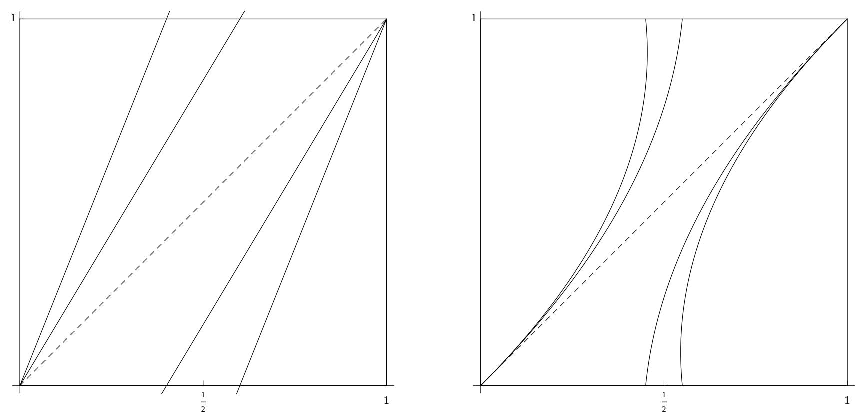

FIGURE 4. On the left, the linear model, $\tilde{\beta}_a$ for r^2. On the right, the suggested qualitative model $\hat{g}$.

homeomorphism, the function defined by following the itinerary of c will be a homeomorphism, establishing the relation between J and each of a collection of arcs indexed by the Cantor set. Observing that $m(a)$ is the same regardless of c, then $\{m(x,c)|x \in J, c \in \mathcal{C}\}$ is a cone over a Cantor set. □

Remark 4.2. As the theorem may be applied on $[0,1]$ about both 0 and 1, $\varprojlim\{[0,1], \tilde{\beta}_a\}$ contains a symmetric pair of cones over Cantor sets.

Remark 4.3. If we consider p to be the positive fixed point of the Ruelle plot r^2, we may apply the theorem to $M = \varprojlim\{[-p,p], r^2\}$. M contains a pair of cones over a Cantor set, as the theorem can be applied to the symmetric branchings about $\pm p$.

Remark 4.4. The fact that r^2 maps an interval around 0 to both an interval containing p and another containing $-p$ suggests that the structure of M is very complicated. Under iteration, neighborhoods of $-p$ will expand while migrating toward the neighborhood of p. After approaching 0, the images may follow either the upper or the lower branch to a neighborhood of $\pm p$. Consequently, periodic points of all periods exist and sets may be constructed that limit on them. This is an area of interest for further work, but is beyond the scope of the present paper.

5. Extensions of Interest

One method to progress in this vein is a change of the domain. Note that $\tilde{\beta}_a(a) = \tilde{\beta}_a(1-a) = \{0, 1\}$, and similarly for r^2. If we identify 0 and 1, then rather than u.s.c. maps acting on $[0, 1]$, we are instead interested in u.s.c. maps on S^1—this time with connected graphs. The identification in the domain means that the binary representations of points in $\mathcal{C}$ are also identified. Consequently, the inverse limits for both $\tilde{\beta}_a$ and r^2 are difficult to picture. As each u.s.c. map contains homeomorphisms fairly close to the squaring map, it seems likely that the inverse limit contains, at the very least, a copy of the dyadic solenoid with a cross section identified as a single point. This diverges significantly from our interest in the cross section of the Lorenz attractor, but it seems an area for further exploration.

It may also be of interest to explore whether the u.s.c. inverse systems obtained through these techniques more closely resemble the attractor approximated numerically. The techniques can also be extended to examine u.s.c. inverse systems accounting for numerical error by replacing the point images in a continuous map with intervals of small diameter (relative to the error bounding, that is). Finally, the disconnected graph seems to have been a key element of this exploration, and the author has observed such in Ruelle plots of other systems near hyperbolic points. It would be of interest to know what behaviors this characterizes and what may be said using the u.s.c. inverse system tool, which allows for this possibility.

References

[1] Marcy Barge, *Horseshoe maps and inverse limits*, Pacific J. Math. **121** (1986), no. 1, 29–39.

[2] Robert L. Devaney, *An Introduction to Chaotic Dynamical Systems.* Menlo Park, CA: The Benjamin/Cummings Publishing Co., Inc., 1986.

[3] John Guckenheimer and Philip Holmes, *Nonlinear Oscillations, Dynamical Systems, and Bifurcations of Vector Fields.* Applied Mathematical Sciences, 42. New York: Springer-Verlag, 1983.

[4] Sarah E. Holte, *Generalized horseshoe maps and inverse limits*, Pacific J. Math. **156** (1992), no. 2, 297–305.

[5] William T. Ingram and William S. Mahavier, *Interesting dynamics and inverse limits in a family of one-dimensional maps*, Amer. Math. Monthly **111** (2004), no. 3, 198–215.

[6] ______, *Inverse limits of upper semi-continuous set valued functions*, Houston J. Math. **32** (2006), no. 1, 119–130.

[7] Thomas Lofaro, *A model of the dynamics of the Newton-Leipnik attractor*, Internat. J. Bifur. Chaos Appl. Sci. Engrg. **7** (1997), no. 12, 2723–2733.

[8] Edward N. Lorenz, *Deterministic nonperiodic flow*, J. Atmospheric Sci. **20** (1963), 130–141.

Department of Mathematics; Guilford College; Greensboro, North Carolina 27410

E-mail address: bmarlin@guilford.edu